COMPOSITE PLASMONIC WAVEGUIDES

Prof. Alina Karabchevsky, www.alinakarabchevsky.com

Integrated Photonics Course 377-2-5599

School of ECE

Ben-Gurion University of the Negev, Israel

OUTLINE

Introduction

Surface plasmon

- Extended surface plasmon
- Localized surface plasmon

Composite-Plasmonic waveguide

- First step $z = 0$
- Second step $z = L$

Invisibility cloaking scheme on composite plasmonic waveguides

Bibliography

INTRODUCTION

- The SPR is a quantum electromagnetic (EM) phenomenon arising from the interaction of light with free electrons at a metal-dielectric interface emerging as a longitudinal EM wave in a two-dimensional gas of charged particles such as free electrons in metals.
- Under certain conditions the energy carried by the photons is transferred to collective excitations of free electrons, called surface plasmons (SPs), at that interface.
- This transfer of energy occurs only at a specific resonance wavelength of light when the momentum of the photon matches that of the plasmon.

THE CONDITIONS FOR EXTENDED SP

The conditions for the extended surface plasmon excitation are:

1. Incident light is TM polarized.
2. The real part of the dielectric constant of the metal and the dielectric are of opposite sign and satisfy: $\Re\{\varepsilon_m\} < -\varepsilon_a$.
3. Wave vector of the incident light is large enough to satisfy the momentum matching $k_x = k_{SP}$.

TM POLARIZED LIGHT

- Propagating SP waves are excited with TM-polarized EM waves when the component of the k-vector along the metal-dielectric interface matches the SP k-vector. The condition of TM polarization is needed to generate the charge distribution on the metal-dielectric interface.

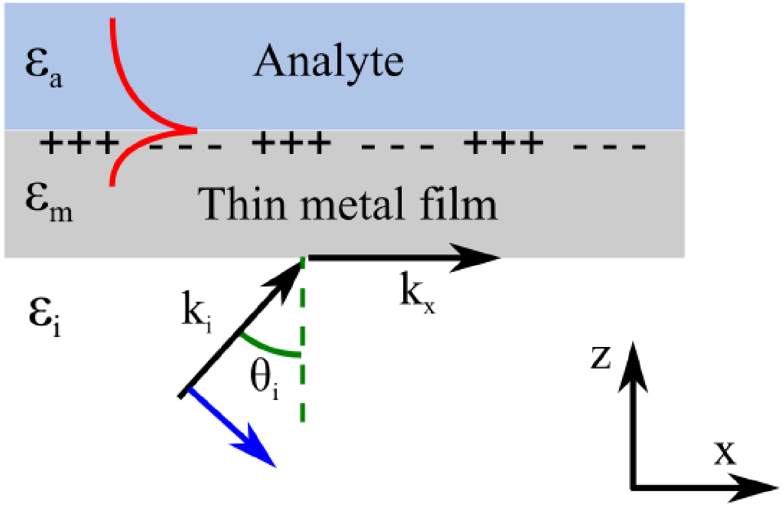

Figure 1: Surface plasmon wave (SPW) excitation at the interface between thin metal film and analyte.

THE DIELECTRIC CONSTANT

- Assuming **TM** plane wave and applying the continuity relations of the tangential field's components (E_x, H_y):

$$E_i(r,t) = (E_{xi}, 0, E_{zi})e^{-k_{zi}|z|}e^{j(k_{xi}x-\omega t)}$$

$$H_i(r,t) = \left(0, H_{yi}, 0\right)e^{-k_{zi}|z|}e^{j(k_{xi}x-\omega t)}$$

$$\frac{k_{zm}}{\varepsilon_m} + \frac{k_{za}}{\varepsilon_a} = 0$$

where ε the relative permittivity and k_z is the z component of the wave vector (k-vector).

THE DIELECTRIC CONSTANT

- Using the phase matching condition $k_{xm} = k_{xa} = k_x$ and the k relation

${k_{zi}}^2 + {k_{xi}}^2 = \varepsilon_j \left(\frac{\omega}{c}\right)^2$, the condition for the **excitation of extended surface plasmon** is defined as:

$$k_x = k_{\mathrm{SP}} = k_i \sqrt{\frac{\varepsilon_m \varepsilon_a}{\varepsilon_m + \varepsilon_a}} \qquad (1)$$

Since for metal $\varepsilon_m < 0$, then $|\varepsilon_m| > \varepsilon_a$.

- From $k_x = k_i n_i \sin(\theta_i)$ we can calculate the angle for SPR ($\theta_{\mathrm{SPR}} = \theta_i$). i - the incident angle in the coupling medium.

PENETRATION DEPTH

- **Penetration depth** δ_a is the depth at which the intensity decays to $1/e$ of the maximum intensity. It equals to $\Im\{k_{zm}\}/2$

$$\delta_a = \frac{\lambda}{2\pi}\sqrt{\frac{\varepsilon_a + \varepsilon_{mr}}{-{\varepsilon_a}^2}} \quad (2)$$

- The penetration depth in the near-infrared (NIR) range is larger by a factor of 8 than that in the visible, although the wavelength ratio is only 2.5. The reason for that is the difference in the real part of the metal dielectric function.

PROPAGATION LENGTH

Propagation length is the distance at which the intensity decays to $1/e$ of the maximum intensity. It equals to $\Im\{k_x\}/2$

$$L_x = \frac{\lambda}{2\pi}\left(\frac{{\varepsilon_{mr}}^2}{\varepsilon_{mi}}\right)\left(\frac{\varepsilon_a + \varepsilon_{mr}}{-{\varepsilon_a}^2}\right)^{\frac{3}{2}} \quad (3)$$

where ε_{mr} and ε_{mi} are the real and the imaginary part of the metal dielectric constant.

DISPERSION CURVES

- Extended surface plasmon on a flat metal/dielectric interface cannot be excited directly by light since $k_{\mathrm{SP}} > k_i$, prohibiting phase-matching.
- The phase-matching between light and SPPs can be achieved by adding a coupling medium. For large frequencies close to ω_p the damping is negligible due to the product $\omega\tau \gg 1$ and then $\varepsilon(\omega)$ is predominantly real.
- Here, the coupling medium allows for the phase matching. The graph shows the dispersion curves for incident light into the metal from vacuum and SF11 at incidence angle of 50 degrees.

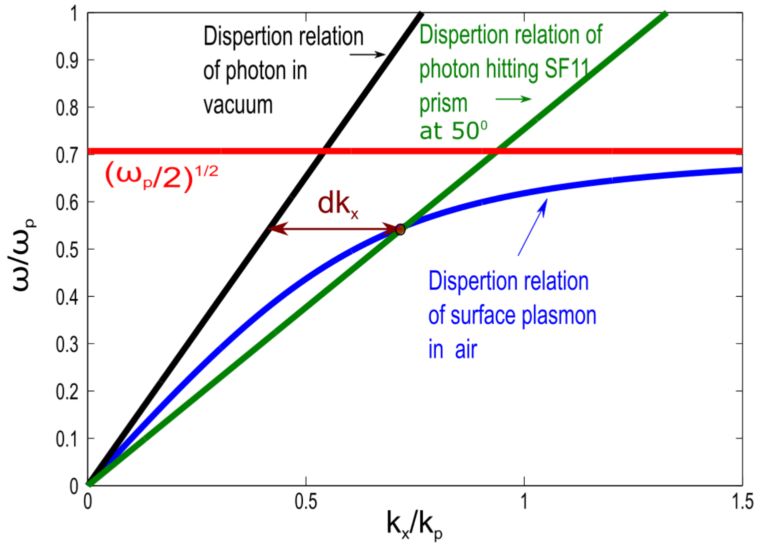

CONFIGURATIONS FOR EXTENDED SPR EXCITATION

Three common configurations:

- Otto configuration.
- Kretschmann-Raether configuration.
- Grating configuration.

OTTO CONFIGURATION

- In Otto configuration there is an air between the prism and the metal layer and the plasmon propagates on the surface of the metal film.

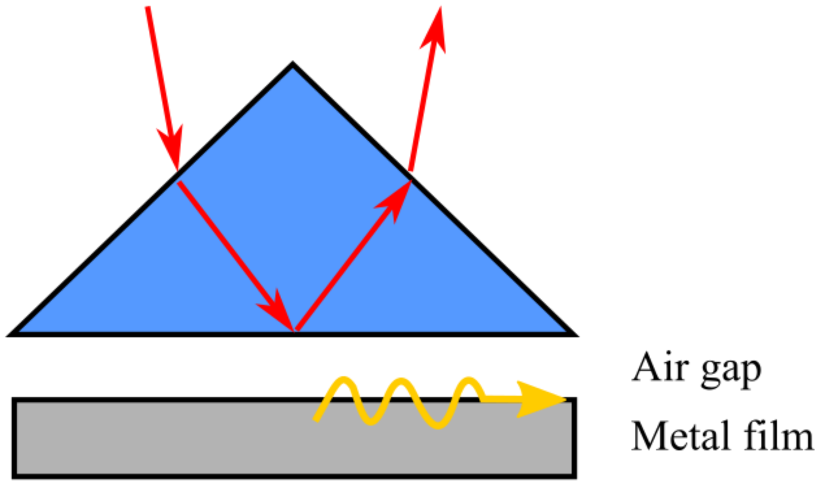

Figure 3: Illustration of Otto configuration for SPR excitation.

KRETSCHMANN-RAETHER CONFIGURATION

- In Kretschmann-Raether configuration, the metal layer is deposited on the prism and the plasmon propagates on the metal-air boundary.

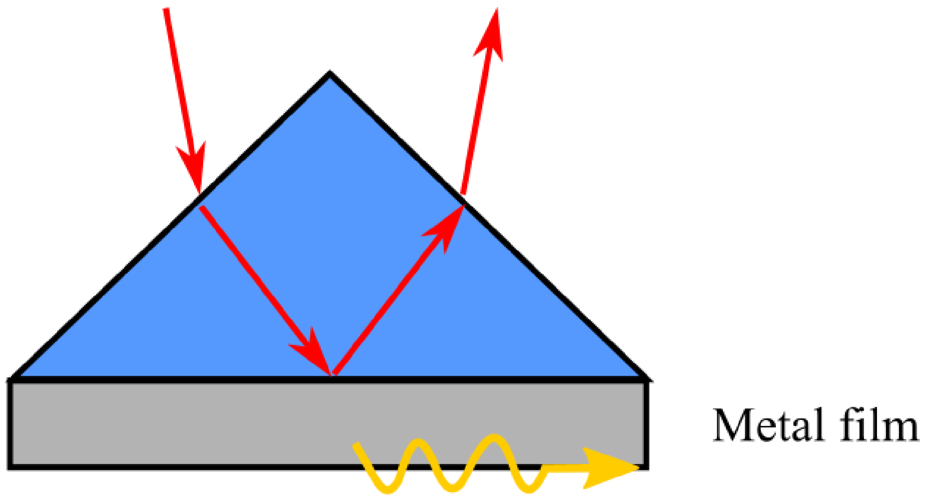

Figure 4: Illustration of basic Kretschmann-Raether configuration for SPR excitation.

GRATING CONFIGURATION

Another option is to excite plasmon by using a metal grating.

Note: The grating can be dielectric on metal substrate or metallic on dielectric substrate.

GRATING CONFIGURATION

In order to excite plasmon in the grating, the matching between the grating constant, the incident light and the plasmonic wave is needed:

$$\frac{2\pi}{\lambda} n_a \sin\theta \pm \frac{2\lambda}{\Lambda} m = \frac{2\pi}{\lambda}\sqrt{\frac{\varepsilon_m \varepsilon_{a,s}}{\varepsilon_m + \varepsilon_{a,s}}} \quad (4)$$

where Λ is the grating constant and a, s corresponds to the medium where the plasmonic wave will propagate (analyte or substrate).

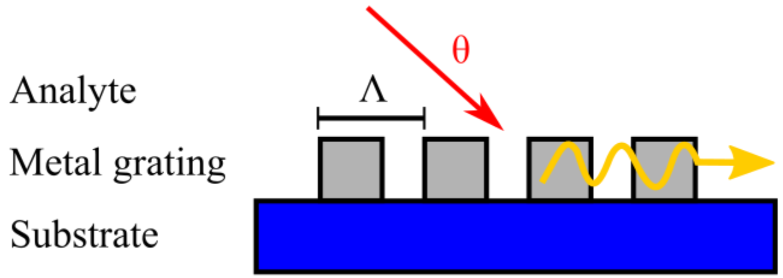

Figure 5: Illustration of grating configuration for SPR excitation.

GRATING EXPERIMENT

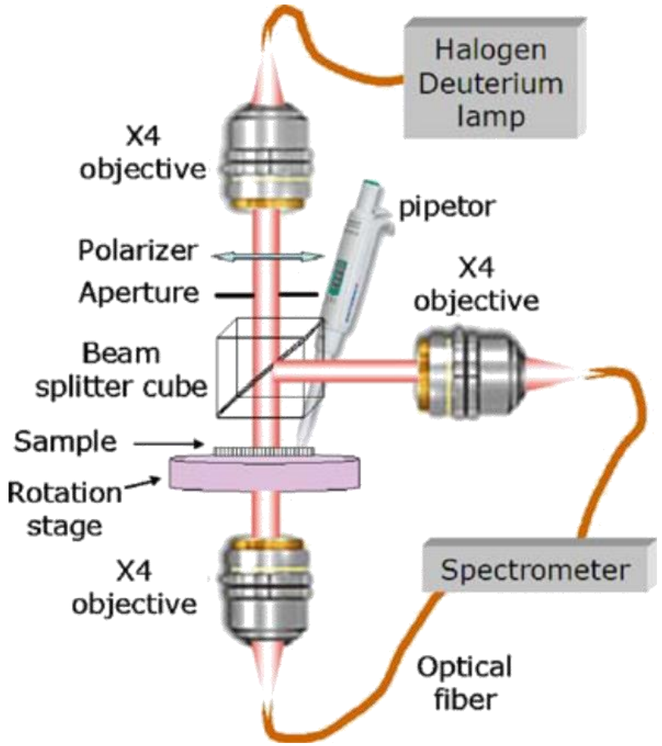

Figure 6: Schematic of the experimental setup of grating configuration for SPR excitation [1]

Alina Karabchevsky, Olga Krasnykov, Mark Auslender, Benny Hadad, Adi Goldner, and Ibrahim Abdulhalim. Theoretical and experimental investigation of enhanced transmission through periodic metal nanoslits for sensing in water environment. Plasmonics, 4(4):281, 2009.

GRATING FABRICATION

(a) Transmission spectra of the Ag grating covered by $d_{\text{Au}} = 5$ nm, for different analytes composed of ethanol diluted in DI water.

(b) zoom on the gray area in the gray box of a. the legend is the same for a and b.

(c) Wavelength as a function of refractive index of ethanol concentrations diluted in DI of resonance presented in (b) and its evaluated regression line. [1]

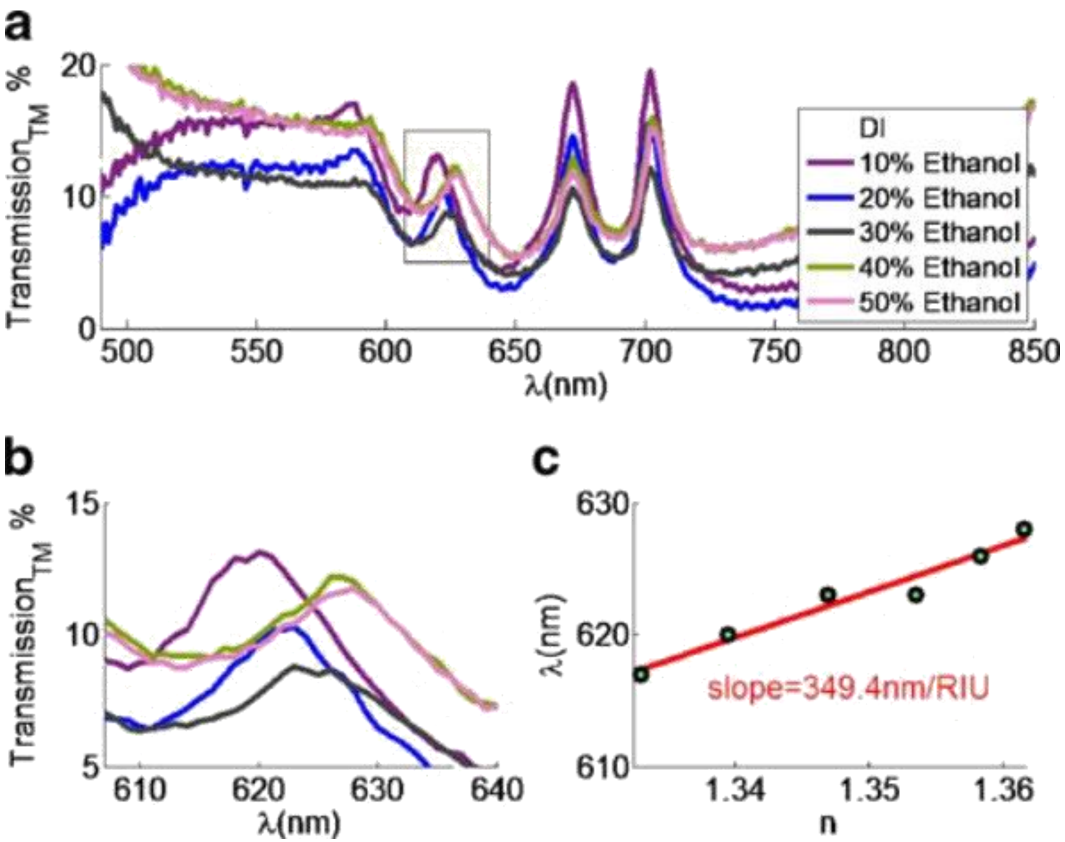

Alina Karabchevsky, Olga Krasnykov, Mark Auslender, Benny Hadad, Adi Goldner, and Ibrahim Abdulhalim. Theoretical and experimental investigation of enhanced transmission through periodic metal nanoslits for sensing in water environment. Plasmonics, 4(4):281, 2009.

LOCALIZED SURFACE PLASMON (LSP)

- When the metal layer made of subwavelength ($d \ll \lambda$) structural units (such as nanoparticles, containing nanoholes, etc.), the plasmon becomes localized and non-propagating. It can't propagate more than the size of the structural unit.

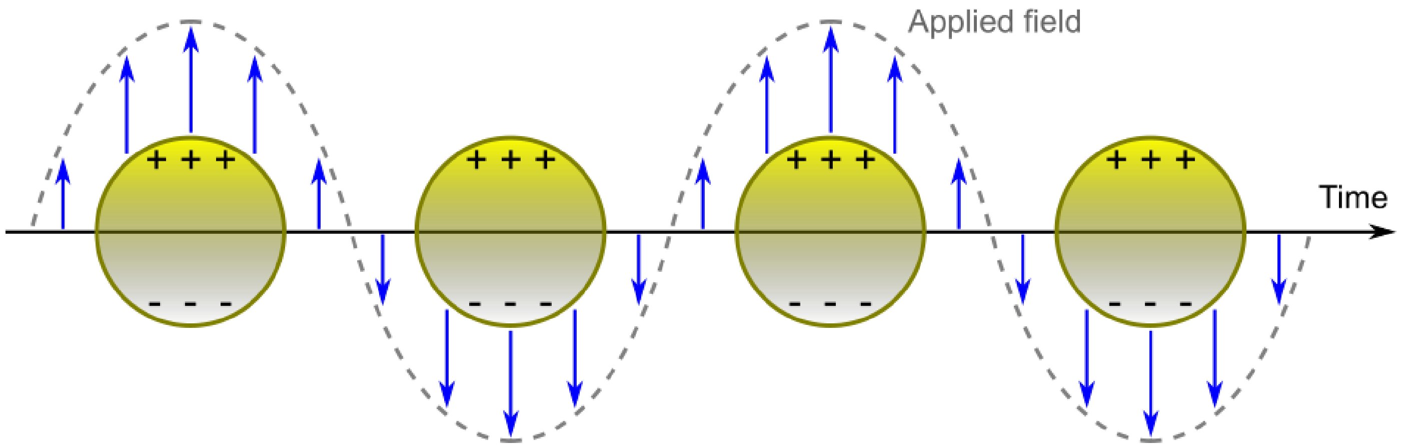

Figure 8: Oscillations of free electrons at the surface of a nanosphere due to applied electric field with arbitrary polarization.

HYBRID PLASMONIC DEVICES

- Hybrid plasmonic devices incorporating dielectric and metallic waveguiding structures offer great potential for ultra-compact high-performance devices from polarizers and sensors, through surface-enhanced Raman spectrometers, to telecommunications filters and all-optical switches. In particular there is growing interest in such plasmonic technologies for biochemical analysis in clinical point-of-care applications.
- Surface plasmon-polaritons (SPP) are supported by several different optical waveguide configurations. Thin metal films sandwiched between two semi-infinite dielectric media are known to support bound and a leaky SPP modes with symmetric and anti-symmetric transverse-magnetic field distributions across the film thickness.

HYBRID PLASMONIC DEVICES

- Hybrid plasmonic devices can be used for variety of applications such as polarizers, filters, modulators and switches.

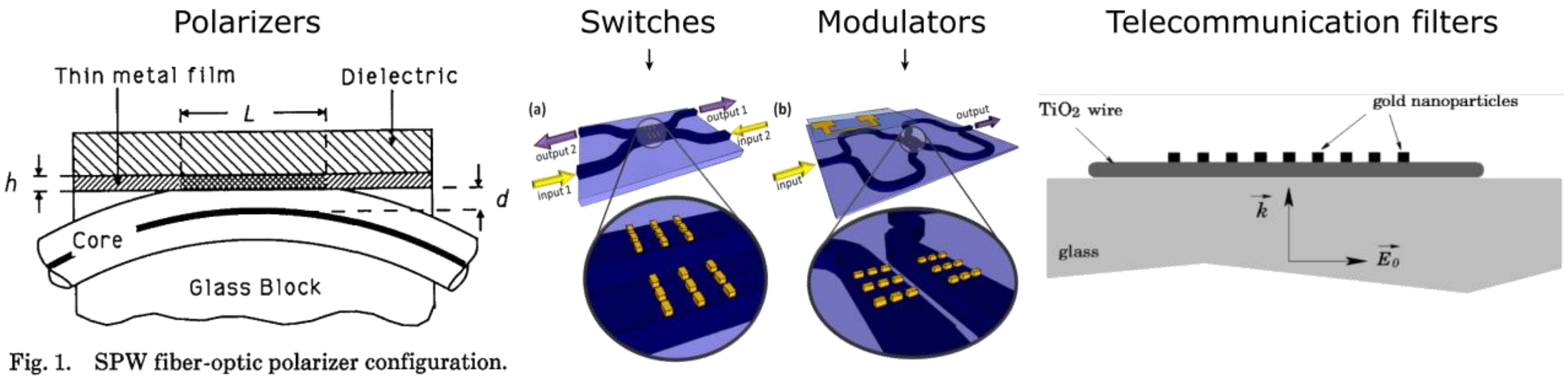

Figure 9: Hybrid plasmonic devices incorporating dielectric and metallic guided wave structures.

THE STRUCTURE

- Here we consider the 3D composite plasmonic waveguide which is modeled throughout at a wavelength of 633 nm [2].
- It consists of a dielectric ridge waveguide with core having index of $n_1 = 1.478$, width of 4 µm and height of 2 µm, covered by a 50 nm thick gold stripe with complex index of $0.197 - 3.466j$ over a finite length L, the refractive index of the substrate $n_2 = 1.471$. The superstrate index was chosen to vary from 1.3 to 1.44.

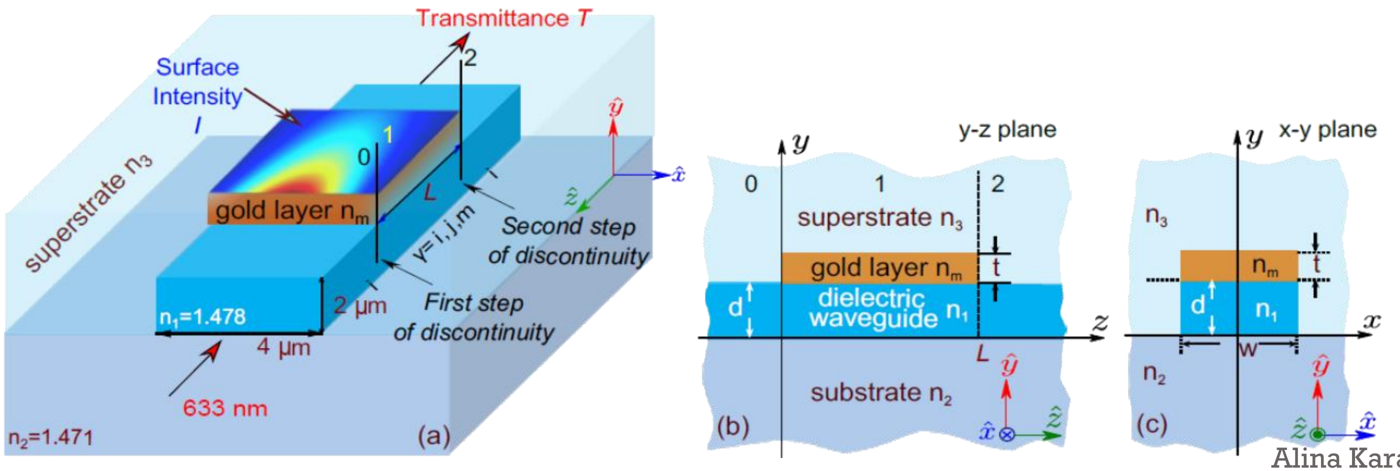

Alina Karabchevsky, James S Wilkinson, and Michalis N Zervas. Transmittance and surface intensity in 3d composite plasmonic waveguides. Optics express, 23(11):14407-14423, 2015.

OPTICAL THEOREM AND COMPLEX INDEX OF REFRACTION

- The index of refraction is linearly related to the forward scattering amplitude

$$n = 1 + 2\pi N k^{-2} S(0)$$

Forward scattering amplitude $S(0)$ of a medium having N particles per unit volume and reduced wavenumber of light is $k_d = \frac{\omega}{c} = 2\pi(n + j\kappa)/\lambda_0$. Using $\sigma_{\text{tot}} = \sigma_{\text{ext}} = 4\pi N k^{-1} \mathcal{L} S(0)$ we obtain relation of dispersion of light by Kramers-Kronig (KK) considering causal propagation of radiation in a medium.

- The dispersion relation

$$\mathcal{R}S(0,\omega) = \frac{1}{2\pi^2 C} \mathcal{P} \int_0^\infty \frac{\omega' \sigma_{\text{tot}}(\omega')}{\omega'^2 - \omega^2} d\omega'$$

This is the Hilbert transform relation between the real and the imaginary parts of the refractive index as a function of frequency.

KRAMERS-KRONIG RELATIONS

Kramers-Kronig relation can be used to calculate the complex refractive index of a material.

$$n(\omega) - 1 = \frac{2}{\pi}\mathcal{P}\int_0^\infty \frac{\omega'\kappa(\omega')}{\omega'^2 - \omega^2}d\omega' \quad (5)$$

$$\kappa(\omega) = -\frac{2\omega}{\pi}\mathcal{P}\int_0^\infty \frac{n(\omega') - 1}{\omega'^2 - \omega^2}d\omega' \quad (6)$$

where $\mathcal{P}$ is the Cauchy principal value and the complex refractive index is $\tilde{n} = n + j\kappa$.

DISPERSION OF A MEDIUM

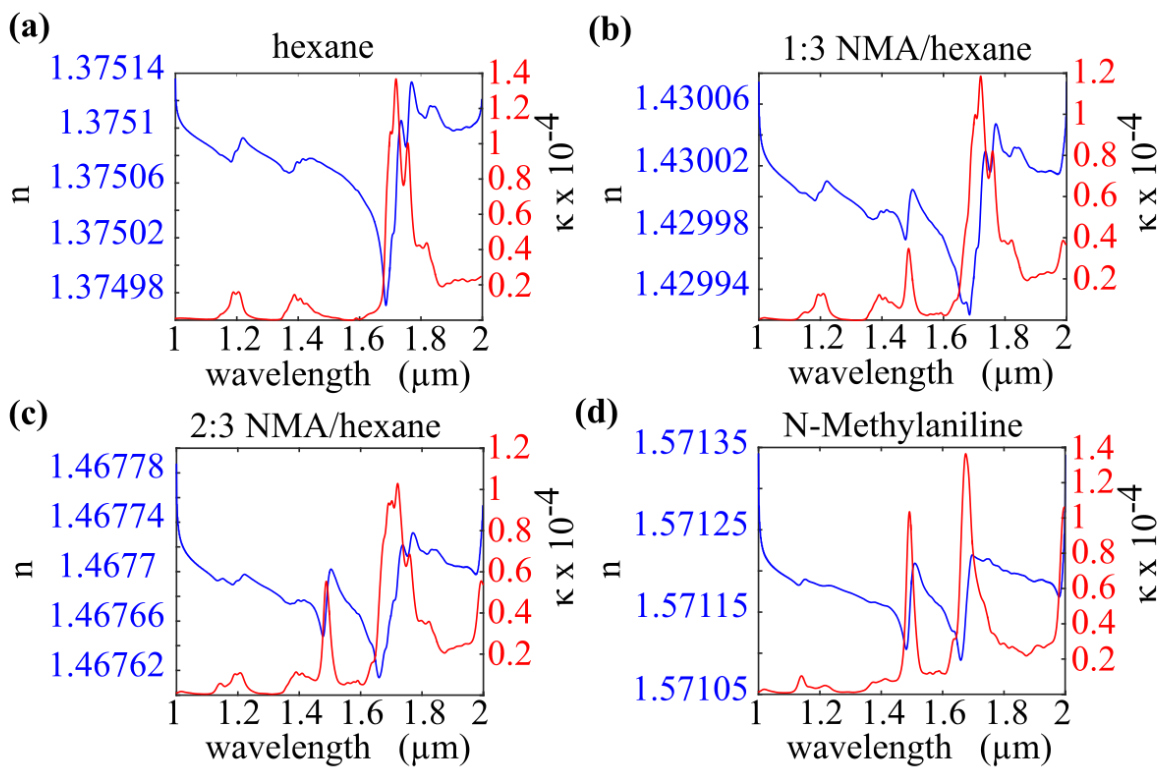

Figure 11: Dispersions calculated by using the KK relations.

H.W.

1. Derive the KK dispersion relation between forward scattering amplitude and the total cross-section.
2. Derive the KK dispersion relation between refractive index and extinction coefficient.
3. Why imaginary part of complex optical index is named extinction coefficient?
4. Why the real part of complex optical index has geometrical meaning?
5. Explain the physical meaning of the causality in Eq. (5).

MODAL COUPLING ACROSS DISCONTINUITIES IN WAVEGUIDES

The discontinuity in the waveguide will produce a reflected guided mode E_r and forward E_{fr} and backward E_{br} traveling radiation modes as well as the transmitted guided mode E_t. The continuity of the electromagnetic fields across the discontinuity will then give, for TE modes

$$E_i + E_r + E_{br} = E_t + E_{fr} \qquad (7)$$

where i, r, t are incident, reflected and transmitted guided modes, respectively. fr and br are forward $S(0)$ and backward $S(\pi)$ scattered radiation modes. Only E_i represents a single mode.

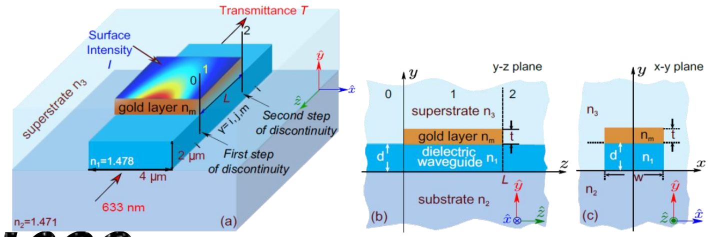

FIELD DISTRIBUTIONS - $z = 0\ \mu m$

The general complex field distributions at the boundary between input waveguide and waveguide with gold overlayer, while ignoring reflected and radiated modes, are:

$$E_{xi0} = \sum_{\gamma=i,j,m} E_{x\gamma 1} \qquad E_{yi0} = \sum_{\gamma=i,j,m} E_{y\gamma 1} \qquad (8,9)$$

$$H_{xi0} = \sum_{\gamma=i,j,m} H_{x\gamma 1} \qquad H_{yi0} = \sum_{\gamma=i,j,m} H_{y\gamma 1} \qquad (10,11)$$

$\boldsymbol{E} = E_x\hat{x} + E_y\hat{y} + E_z\hat{z}$ and $\boldsymbol{H} = H_x\hat{x} + H_y\hat{y} + H_z\hat{z}$. $\hat{x}$, $\hat{y}$ and $\hat{z}$ are unit vectors in the x, y and z directions, respectively.

BONUS

The task:

1. Derive transmittance and surface intensity while considering reflected and radiated modes.

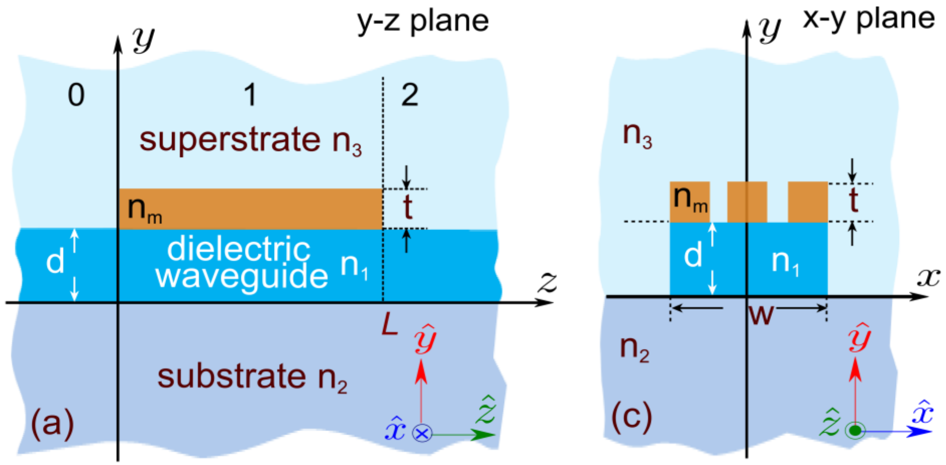

Figure 12: Plasmonic grating overlayer.

CROSS-SECTIONS OF ε_y

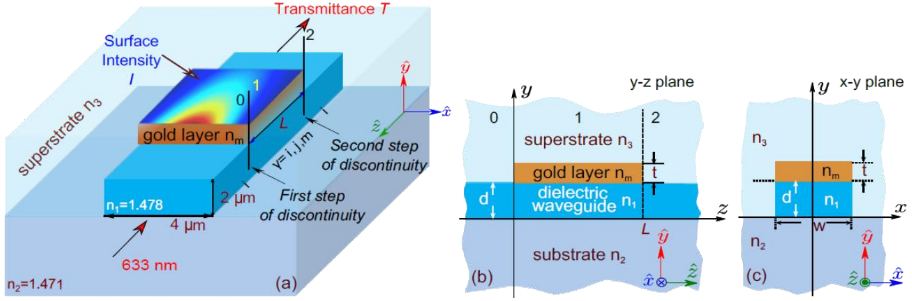

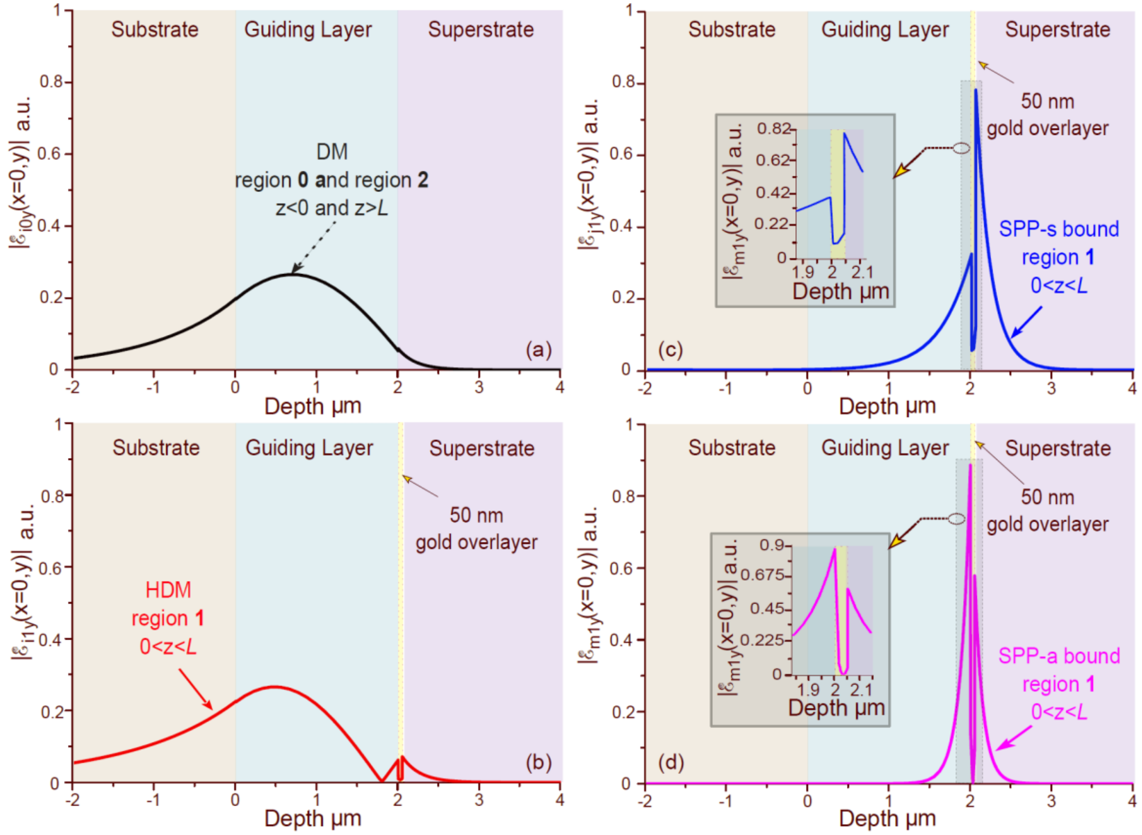

Figure 13: Cross-sections of the y-component of the electric field magnitude for the structure shown in Fig. 10 with a superstrate index of 1.4 for different regions [2].

Alina Karabchevsky, James S Wilkinson, and Michalis N Zervas. Transmittance and surface intensity in 3d composite plasmonic waveguides. Optics express, 23(11):14407-14423, 2015.

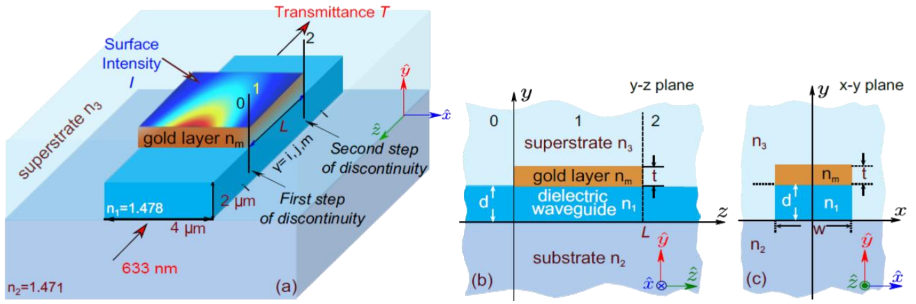

MODE-MATCHING

$$E_{\xi i0} = \sum_{\gamma=i,j,m} E_{\xi\gamma 1} \qquad H_{\xi i0} = \sum_{\gamma=i,j,m} H_{\xi\gamma 1} \tag{12}$$

where $\xi = x, y$. An expression for the expansion coefficient between input mode $i0$ in region 0 and mode $j1$ in region 1 is derived using the complex orthogonality principle:

$$\frac{\iint_{-\infty}^{\infty}\left[\left(\mathbf{E}_{i0}\times\mathbf{H}_{\gamma 1}\right)_z + \left(\mathbf{E}_{\gamma 1}\times\mathbf{H}_{i0}\right)_z\right]dxdy =}{\iint_{-\infty}^{\infty}\left[\left(\mathbf{E}_{\gamma 1}\times\mathbf{H}_{\gamma 1}\right)_z + \left(\mathbf{E}_{\gamma 1}\times\mathbf{H}_{\gamma 1}\right)_z\right]dxdy} \tag{13}$$

where $\gamma 1 = i1, j1, m1$.

EXPRESSION OF THE EXPANSION COEFFICIENTS

- To derive the expression of the expansion coefficient between input mode i at the 0 side of the first step and mode j at the gold coated side of the first step 1.

Multiplying Eq. (8) by H_{yj1} and Eq. (9) by H_{xj1} and subtracting between them leads to:

$$E_{xi0}H_{yj1} - E_{yi0}H_{xj1} = E_{xj1}H_{yj1} - E_{yj1}H_{xj1} \qquad (14)$$

Multiplying Eq. (10) by E_{yj1} and Eq. (11) by E_{xj1} and subtracting between them leads to:

$$-\left(E_{yj1}H_{xi0} - E_{xj1}H_{yi0}\right) = -(E_{yz1}H_{xj1} - E_{xj1}H_{yj1}) \qquad (15)$$

Which is simply:

$$E_{xj1}H_{yi0} - E_{yj1}H_{xi0} = E_{xj1}H_{yj1} - E_{yj1}H_{xj1} \qquad (16)$$

In Eq. (14)-(16), complex orthogonality principle has been considered. Therefore, $\gamma \neq j$ and $I_{\gamma,j} = 0$ at steps 1 and 2.

POWER CARRIED BY MODE j ON SIDE 1 OF DISCONTINUITY

By adding Eq. (14) and Eq. (16) and integrating over a whole range we obtain power carried in a mode j on the side 1 of the first abrupt step:

$$\iint_{-\infty}^{\infty}\left[\left(\mathbf{E}_{i0}\times\mathbf{H}_{j1}\right)_z+\left(\mathbf{E}_{j1}\times\mathbf{H}_{i0}\right)_z\right]dxdy = \iint_{-\infty}^{\infty}\left[2\left(\mathbf{E}_{j1}\times\mathbf{H}_{j1}\right)_z\right]dxdy \quad (17)$$

General complex electric and magnetic field distribution components:

$$\mathbf{E}_\delta(x,y,z)=a_\delta\bar{\mathcal{E}}_\delta(x,y)\exp(-j\beta_\delta z) \quad (18)$$

$$\mathbf{H}_\delta(x,y,z)=a_\delta\bar{\mathcal{H}}_\delta(x,y)\exp(-j\beta_\delta z) \quad (19)$$

where $z=0$ at the first step, β_δ is a propagation constant of mode δ and $\bar{\mathcal{E}}_\delta(x,y)$ and $\bar{\mathcal{H}}_\delta(x,y)$ are extracted complex field components.

RELATION BETWEEN EIGENMODES AT AN ABRUPT STEP

By substituting Eq. (18) and Eq. (19) into Eq. (17) we obtain:

$$a_{i0}a_{\gamma 1}\iint_{-\infty}^{\infty}\left[\left(\bar{\mathcal{E}}_{i0}\times\bar{\mathcal{H}}_{\gamma 1}\right)_z+\left(\bar{\mathcal{E}}_{\gamma 1}\times\bar{\mathcal{H}}_{i0}\right)_z\right]dxdy= \tag{20}$$

$$=\left(a_{\gamma 1}\right)^2\iint_{-\infty}^{\infty}2\left[\left(\bar{\mathcal{E}}_{\gamma 1}\times\bar{\mathcal{H}}_{\gamma 1}\right)_z\right]dxdy=$$

To obtain a relation between eigenmodes at an abrupt step:

$$a_{i0}\left(I_{i0,\gamma 1}+I_{\gamma 1,i0}\right)=a_{\gamma 1}2I_{\gamma 1,\gamma 1}$$

$$a_{\gamma 1}=a_{i0}\frac{I_{i0,\gamma 1}+I_{\gamma 1,i0}}{2I_{\gamma 1,\gamma 1}} \tag{21}$$

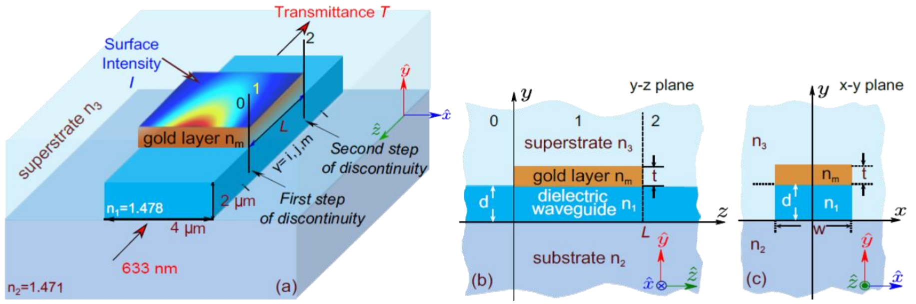

EIGENMODES

where

$$I_{i,\gamma} = \iint_{-\infty}^{\infty} \left[\left(\bar{\mathcal{E}}_i \times \bar{\mathcal{H}}_\gamma \right)_z \right] dxdy = \iint_{-\infty}^{\infty} \left(\mathcal{E}_{xi} \mathcal{H}_{y\gamma} - \mathcal{E}_{yi} \mathcal{H}_{x\gamma} \right) dxdy \quad (22)$$

Let define complex A_δ

$$A_\delta = |A_\delta| \exp(-j\phi_\delta) \quad (23)$$

A_δ is related to the power carried by a mode as:

$$P_\delta = |A_\delta|^2 \quad (24)$$

The aim: each mode carrying power of unity: $P_\delta = 1$

NORMALIZATION OF EIGENMODES

$$a_\delta = N_\delta A_\delta = \frac{E_\delta(x,y,z)}{\mathcal{E}_\delta(x,y)\exp(-j\beta_\delta z)} \tag{25}$$

The normalization factor having unity power:

$$N_\delta = \left(\frac{2}{\Re\left\{\iint_{-\infty}^{\infty}\left(\bar{\mathcal{E}}_i \times \bar{\mathcal{H}}_\gamma^*\right)_z dxdy\right\}}\right)^{1/2} \tag{26}$$

where

$$\bar{\mathcal{E}} = \mathcal{E}_x\hat{x} + \mathcal{E}_y\hat{y} + \mathcal{E}_z\hat{z} \tag{27}$$

$$\bar{\mathcal{H}} = \mathcal{H}_x\hat{x} + \mathcal{H}_y\hat{y} + \mathcal{H}_z\hat{z} \tag{28}$$

NORMALIZATION

We express normalization factor N_δ as:

$$N_\delta = \sqrt{\frac{2}{\Re\{I_{\delta,\delta}\}}} \tag{29}$$

Which is:

$$A_{\gamma 1} N_{\gamma 1} = \frac{A_{\gamma 0} N_{\gamma 0}\left(I_{i0,\gamma 1} + I_{\gamma 1,i0}\right)}{2 I_{\gamma 1,\gamma 1}} \tag{30}$$

Let define expansion coefficient $c_{i0,\gamma 1}$:

$$c_{i0,\gamma 1} = \frac{a_{\gamma 1}}{a_{i0}} = \frac{N_{i0}}{N_{j1}} \cdot \frac{I_{i0,j1} + I_{j1,i0}}{2 I_{j1,j1}} \tag{31}$$

which expands mode i at 0 side into mode j at side 1 of 1^{st} abrupt step.

EXPANSION COEFFICIENT

For $z = 0$:

$$a_{i0}\mathcal{H}_{\xi i0} = \sum_{\gamma=i,j,m} a_{\gamma 1}\mathcal{H}_{\xi\gamma 1} \qquad a_{i0}\mathcal{E}_{\xi i0} = \sum_{\gamma=i,j,m} a_{\gamma 1}\mathcal{E}_{\xi\gamma 1} \tag{32}$$

The power in any region is defined as:

$$P = \frac{1}{2}\Re\left\{\iint_{-\infty}^{\infty}(\mathcal{E}\times\mathcal{H}^*)_z dxdy\right\} \tag{33}$$

An expansion coefficient $c_{i0,\gamma 1}$ expanding mode $i1$ from region 0 into mode $\gamma 1$ in region 1 over the first abrupt step is:

$$c_{i0,\gamma 1} = \frac{a_{\gamma 1}}{a_{i0}} = \frac{N_{i0}}{N_{\gamma 1}} \cdot \frac{I_{i0,\gamma 1} + I_{\gamma 1,i0}}{2I_{\gamma 1,\gamma 1}} \tag{34}$$

EXPANSION COEFFICIENT

At $z = L$, the expansion coefficients are derived in a similar manner to that detailed above resulting in:

$$c_{i1,\gamma 2} = \frac{I_{\gamma 1,j2} + I_{i2,\gamma 1}}{2I_{i2,i2}} \exp\left[-j\left(\beta_{\gamma 2} - \beta_{i1}\right)L\right] \tag{35}$$

Since $a_{\gamma 1} = c_{i0,\gamma 1} a_{i0}$

$$a_{i2} = c_{i0,\gamma 1} a_{i0} c_{\gamma 1,i2} \tag{36}$$

or

$$A_{i2} N_{i2} = c_{i0,\gamma 1} A_{i0} N_{i0} c_{\gamma 1,i2} \tag{37}$$

BONUS

The task:

1. Derive expansion coefficients considering reflection and radiation modes when $z = L$.

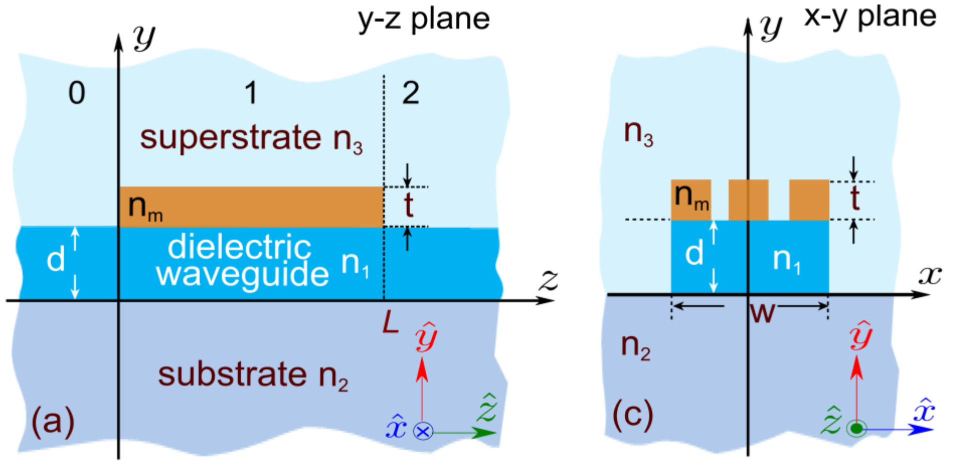

Figure 12: Plasmonic grating overlayer.

SURFACE INTENSITY

where $\mathcal{E}_1$ and $\mathcal{H}_1$

$$\mathcal{E}_1 = \sum_{\gamma=i,j,m} c_{i0,\gamma 1} \mathcal{E}_{\gamma 1} \qquad (38)$$

$$\mathcal{H}_1 = \sum_{\gamma=i,j,m} c_{i0,\gamma 1} \mathcal{H}_{\gamma 1} \qquad (39)$$

$P_1/P_0 < 1$ and surface intensity of, for example, the y component of an electric field (normalized to the complex input field amplitude a_{i0}) is:

$$\text{Intensity} = |E(x, y_s, z)|^2 = \left| \sum_{\gamma=i,j,m} c_{i0,\gamma 1} \mathcal{E}_{y\gamma 1}(x, y_s, z) \right|^2 \qquad (40)$$

where $y_s = d + t$

CALCULATED SURFACE INTENSITY

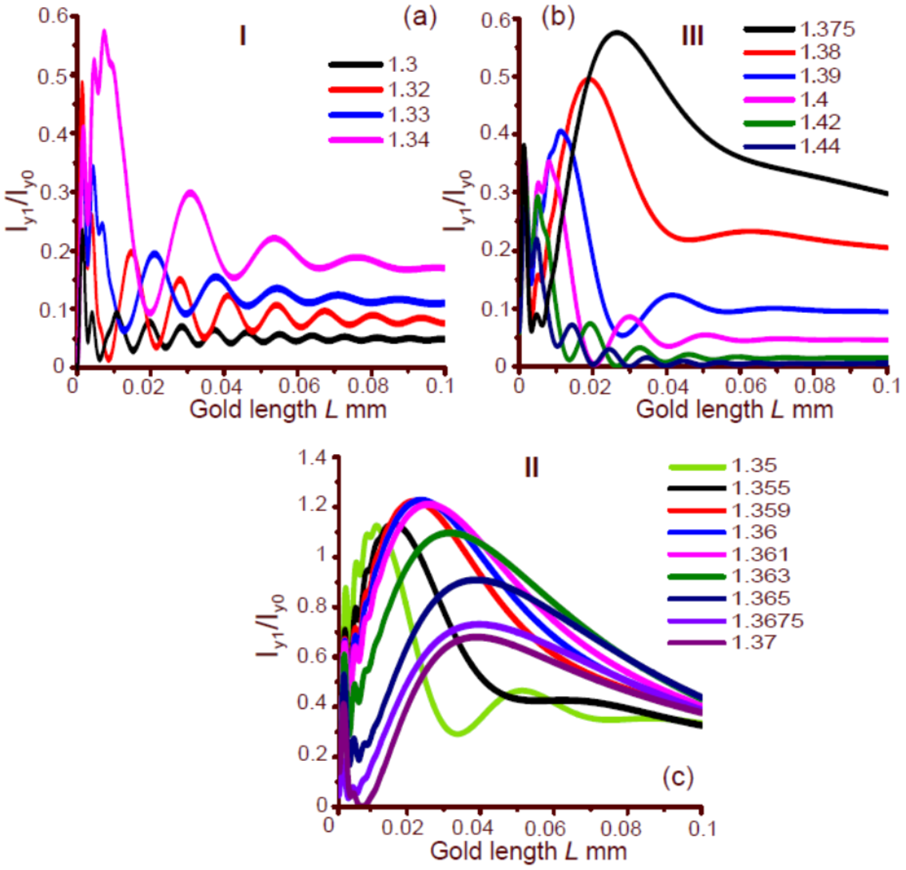

Figure 15: Calculated surface intensity profiles at $x = 0$ and along $L = 100\ \mu m$ [2].

Alina Karabchevsky, James S Wilkinson, and Michalis N Zervas. Transmittance and surface intensity in 3d composite plasmonic waveguides. Optics express, 23(11):14407-14423, 2015.

CALCULATED SURFACE INTENSITY

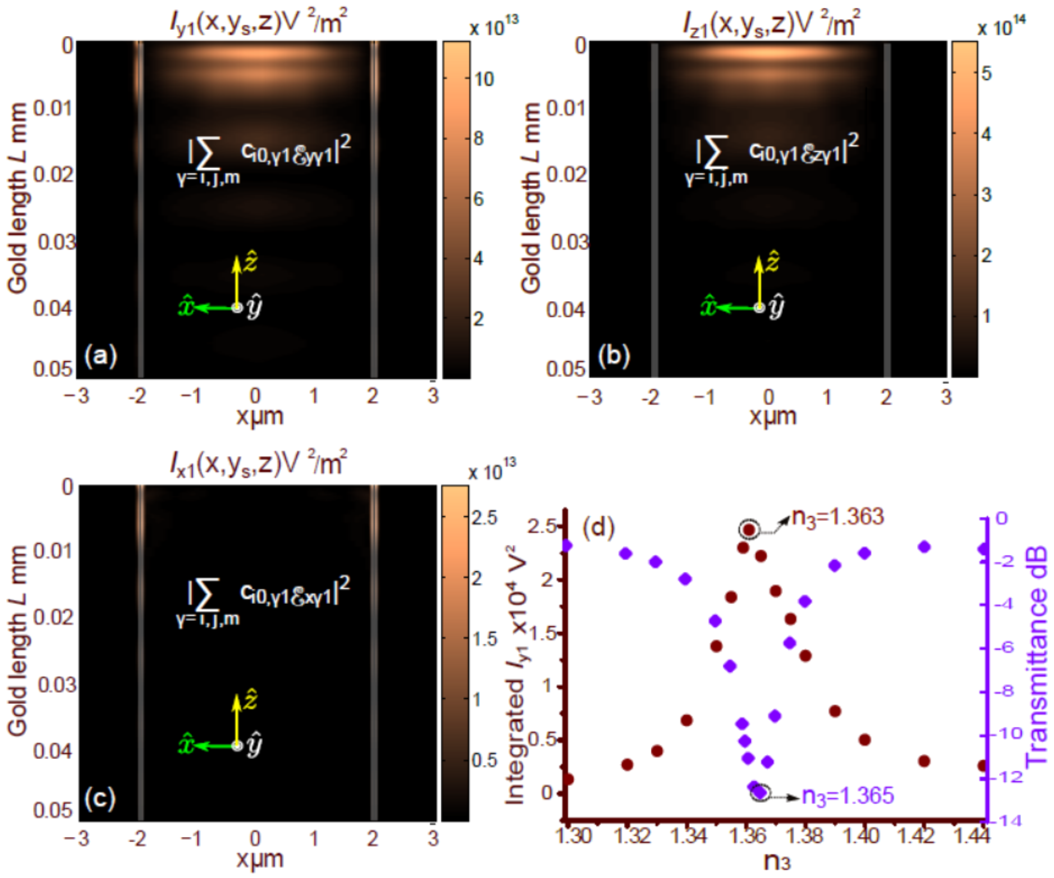

Figure 16: Mapped surface intensity [2].

Alina Karabchevsky, James S Wilkinson, and Michalis N Zervas. Transmittance and surface intensity in 3d composite plasmonic waveguides. Optics express, 23(11):14407-14423, 2015.

FIELD DISTRIBUTIONS - $z = L$

$$E_{xi2} = \sum_{\gamma=i,j,m} E_{x\gamma1} \quad (41)$$

$$E_{yi2} = \sum_{\gamma=i,j,m} E_{y\gamma1} \quad (42)$$

$$H_{xi2} = \sum_{\gamma=i,j,m} H_{x\gamma1} \quad (43)$$

$$H_{yi2} = \sum_{\gamma=i,j,m} H_{y\gamma1} \quad (44)$$

Multiplying Eq. (41) by H_{yi2} and Eq. (42) by H_{xi2} and subtracting between them leads to:

$$E_{x\gamma1}H_{yi2} - E_{y\gamma1}H_{xi2} = E_{xi2}H_{yi2} - E_{yi2}H_{xi2} \quad (45)$$

FIELD DISTRIBUTIONS - $z = L$

Multiplying Eq. (43) by E_{yi2} and Eq. (44) by E_{xi2} and subtracting between them leads to:

$$E_{yi2}H_{x\gamma1} - E_{xi2}H_{y\gamma1} = E_{yi2}H_{xi2} - E_{xi2}H_{yi2} \qquad (46)$$

Then, we are adding Eq. (45) and Eq. (46) and integrating over a whole range to obtain power carried in a mode i on the side 2 of the second step:

$$\iint_{-\infty}^{\infty}\left[\left(E_{\gamma1} \times H_{i2}\right)_z + \left(E_{i2} \times H_{\gamma1}\right)_z\right] dxdy =$$
$$= \iint_{-\infty}^{\infty}[(E_{i2} \times H_{i2})_z + (E_{i2} \times H_{i2})_z]dxdy \qquad (47)$$
$$= \iint_{-\infty}^{\infty} 2[(E_{i2} \times H_{i2})_z]dxdy$$

FIELD DISTRIBUTIONS - $z = L$

The field components as an amplitude and phase at the second step are:

$$E_\delta(x, y, L) = a_\delta \mathcal{E}_\delta(x, y) \exp(-j\beta_\delta L) \tag{48}$$

By substituting Eq. (41) and Eq. (44) into Eq. (47) we obtain:

$$a_{\gamma 1} a_{i2} \exp\left[-j\left(\beta_{\gamma 1} + \beta_{i2}\right)L\right] \iint_{-\infty}^{\infty} \left[\left(\mathcal{E}_{\gamma 1} \times \mathcal{H}_{i2}\right)_z + \left(\mathcal{E}_{i2} \times \mathcal{H}_{\gamma 1}\right)_z\right] dxdy \tag{49}$$

which is equal to:

$$(a_{i2})^2 \exp[-j2\beta_{i2}L] \iint_{-\infty}^{\infty} [(\mathcal{E}_{i2} \times \mathcal{H}_{i2})_z + (\mathcal{E}_{i2} \times \mathcal{H}_{i2})_z] dxdy \tag{50}$$

FIELD DISTRIBUTIONS - $z = L$

by simplifying Eq. (49) = Eq (50), we obtain Eq. (51) = Eq. (52):

$$a_{\gamma 1} \exp[-j\beta_{\gamma 1} L] \iint_{-\infty}^{\infty} \left[\left(\mathcal{E}_{\gamma 1} \times \mathcal{H}_{i2} \right)_z + \left(\mathcal{E}_{i2} \times \mathcal{H}_{\gamma 1} \right)_z \right] dxdy \qquad (51)$$

$$a_{i2} \exp[-j\beta_{i2} L] \iint_{-\infty}^{\infty} [(\mathcal{E}_{i2} \times \mathcal{H}_{i2})_z + (\mathcal{E}_{i2} \times \mathcal{H}_{i2})_z] dxdy \qquad (52)$$

TRANSMITTANCE

$$T = \left|\frac{A_{i2}}{A_{i0}}\right|^2 = \left|\sum_{\gamma=i,j,m} c_{i0,\gamma 1} c_{\gamma 1,i2} \left(\frac{N_{i0}}{N_{i2}}\right)\right|^2$$

$$T = \left|\frac{A_{i2}}{A_{i0}}\right|^2 = \left|\sum_{\gamma=i,j,m} \frac{I_{i0,j1} + I_{j1,i0}}{2I_{j1,j1}} \frac{I_{\gamma 1,i2} + I_{i2,\gamma 1}}{2I_{i2,i2}} \exp(-j\beta_{\gamma 1} L)\right|^2 \qquad (53)$$

Relation of the fields at the second step to calculate the power are:

$$\mathcal{E}_{x\gamma 1} = \sum_{\gamma=i,j,m} c_{\gamma 1,i2} \mathcal{E}_{xi2} \tag{54}$$

$$\mathcal{E}_{y\gamma 1} = \sum_{\gamma=i,j,m} c_{\gamma 1,i2} \mathcal{E}_{yi2} \tag{55}$$

$$\mathcal{H}_{x\gamma 1} = \sum_{\gamma=i,j,m} c_{\gamma 1,i2} \mathcal{H}_{xi2} \tag{56}$$

$$\mathcal{H}_{y\gamma 1} = \sum_{\gamma=i,j,m} c_{\gamma 1,i2} \mathcal{H}_{yi2} \tag{57}$$

SUMMARY

- Theoretical study of planar waveguides with plasmonic overlayer.
- Coupling of hybrid real field distributions over a discontinuity in a waveguide horns.
- Mapping of surface intensity in 3D composite-plasmonic waveguides.
- Optical transmittance follows HDM modal attenuation loss.

ORTHOGONALITY OF COMPLEX MODES

- $\forall i \neq j \qquad I_{i,j} = 0$

$$E_{xi0} = \sum_{\gamma=i,j,m} E_{x\gamma1} \tag{58}$$

$$E_{yi0} = \sum_{\gamma=i,j,m} E_{y\gamma1} \tag{59}$$

$$H_{xi0} = \sum_{\gamma=i,j,m} H_{x\gamma1} \tag{60}$$

$$H_{yi0} = \sum_{\gamma=i,j,m} H_{y\gamma1} \tag{61}$$

MATCHING MODES EQUATIONS

$$\sum_{\gamma=i,j,m} A_{\gamma 1} = \sum_{\gamma=i,j,m} c_{i\gamma} A_{\gamma 0} \tag{62}$$

$$A_{\gamma 2} = \sum_{\gamma=i,j,m} c_{\gamma i} A_{\gamma 1} \tag{63}$$

$$c_{i\gamma} = \frac{I_{i0,\gamma 1} + I_{\gamma 1,i0}}{2I_{\gamma 1,\gamma 1}} \sqrt{\frac{\Re\{I_{\gamma 1,\gamma 1}\}}{\Re\{I_{i0,i0}\}}} \tag{64}$$

$$c_{\gamma i} = \frac{I_{\gamma 1,i2} + I_{i2,\gamma 1}}{2I_{i2,i2}} \sqrt{\frac{\Re\{I_{\gamma 1,\gamma 1}\}}{\Re\{I_{i0,i0}\}}} \tag{65}$$

Note: $I_{i2,i2} = I_{i0,i0} \quad \Rightarrow \quad I_{\delta,\delta} = \iint_{-\infty}^{\infty} (\bar{\mathcal{E}}_\delta \times \bar{\mathcal{H}}_\delta)_z \, dxdy$

NUMERICAL APPROACH

Figure 17: Cross-sections of the y-component of the electric field magnitude for the structure with a superstrate index of 1.4 in (a) a purely dielectric mode (DM) in a dielectric waveguide in the $z < 0$ and $z > L$ regions [2].

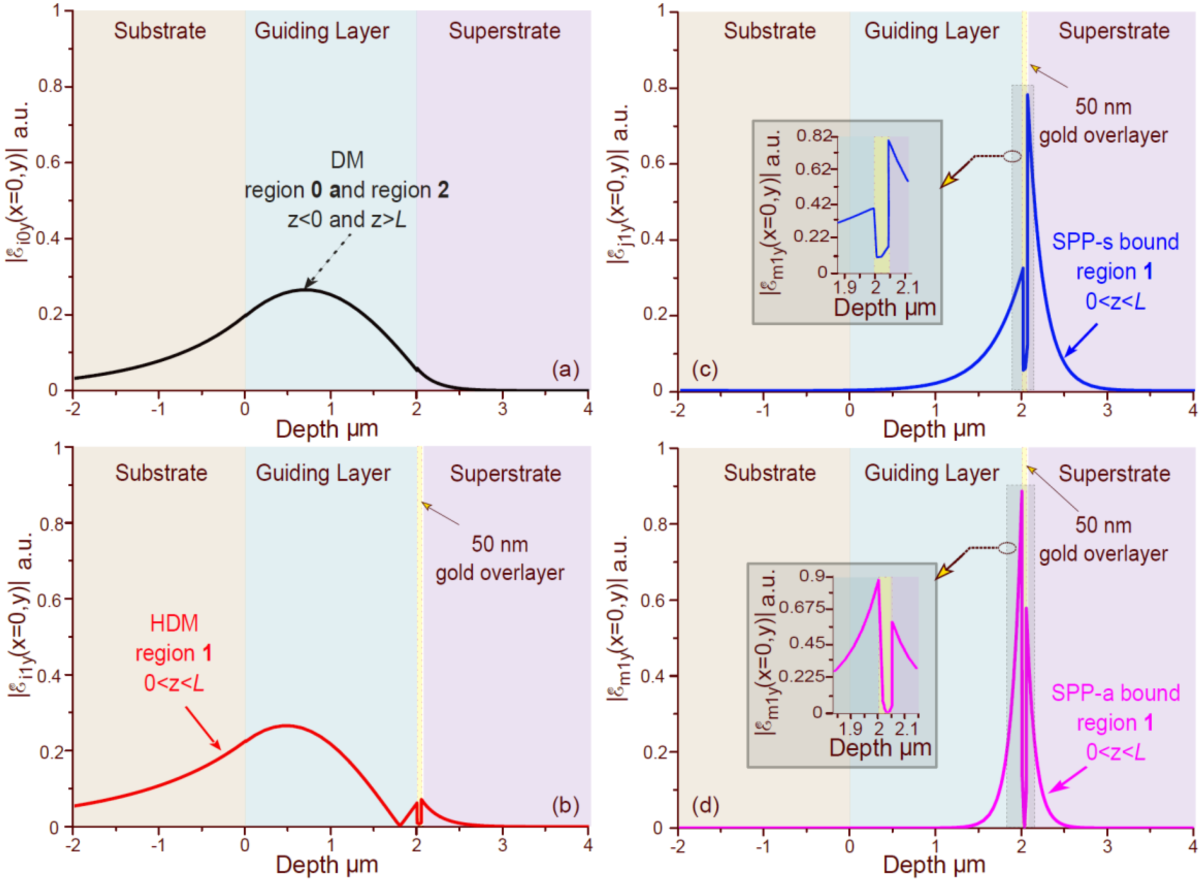

Alina Karabchevsky, James S Wilkinson, and Michalis N Zervas. Transmittance and surface intensity in 3d composite plasmonic waveguides. Optics express, 23(11):14407-14423, 2015.

MODES

- Evolution of the dominant y-component of electric field magnitudes for quasi-transverse magnetic modes at resonance having superstrate index of 1.365, and far from it, at low superstrate index: 1.3 and high superstrate index 1.44 as labeled on the figure accordingly for DM, HDM, SPP-s and SPP-a guided modes [2].

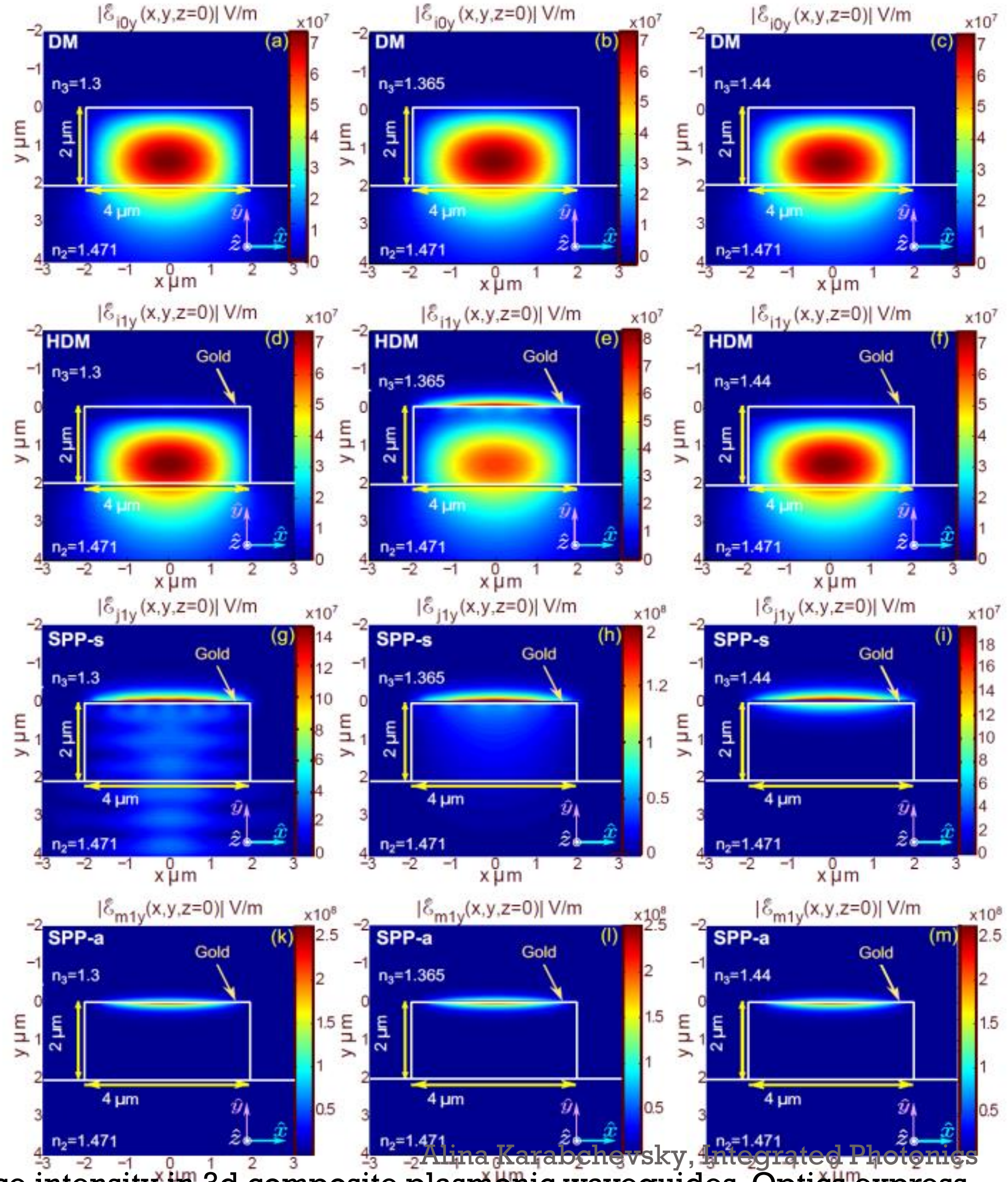

Alina Karabchevsky, James S Wilkinson, and Michalis N Zervas. Transmittance and surface intensity in 3d composite plasmonic waveguides. Optics express, 23(11):14407-14423, 2015.

ANALYSIS OF COMPLEX N_{eff}

Effective refractive index RIU:

$$N_{\text{eff}} = \Re\{\beta\}\lambda/2\pi \qquad (66)$$

Modal attenuation coefficient dB/cm:

$$\alpha = 0.2\log(e)\,\Im\{\beta\} \qquad (67)$$

ANALYSIS OF COMPLEX N_{eff}

Figure 18: Variation of (a) effective refractive indices and (b) modal attenuation coefficients a in the gold-coated region $0 < z < L$ with n_3; (c) zoomed effective indices in the region enclosed in (a) [2].

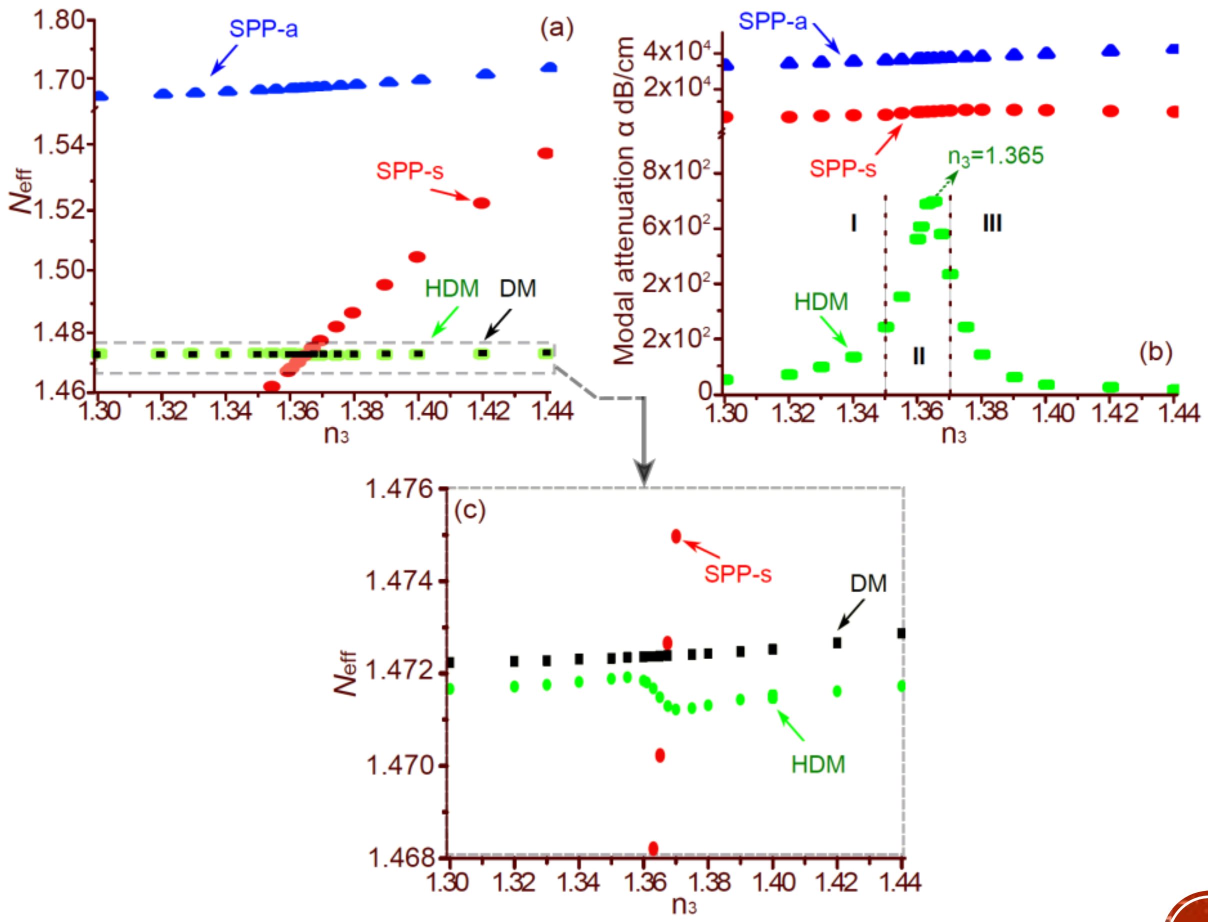

Alina Karabchevsky, James S Wilkinson, and Michalis N Zervas. Transmittance and surface intensity in 3d composite plasmonic waveguides. Optics express, 23(11):14407-14423, 2015.

PREDICTION OF TRANSMITTANCE

Transmittance dB:

$$T = \left| \sum_{\gamma=i,j,k} \frac{\left(I_{i0,\gamma1} + I_{\gamma1,i0}\right)^2}{4 I_{i0,i0} I_{\gamma1,\gamma1}} \exp\left(-j\beta_{\gamma1} L\right) \right|^2 \quad (68)$$

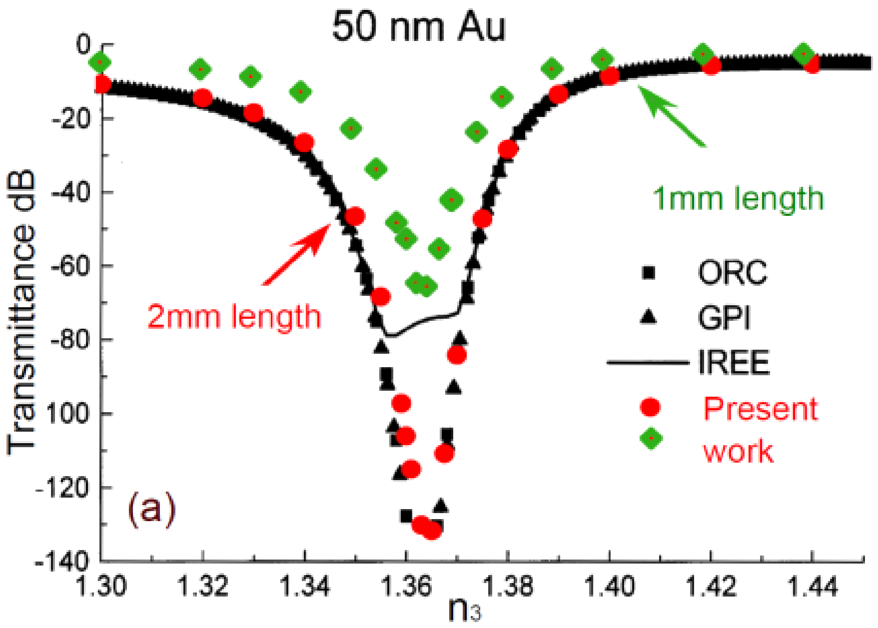

Figure 19: Calculated optical transmittance for $L = 2$ mm based on our model and of $L = 1$ mm [2].

Alina Karabchevsky, James S Wilkinson, and Michalis N Zervas. Transmittance and surface intensity in 3d composite plasmonic waveguides. Optics express, 23(11):14407-14423, 2015.

SURFACE INTENSITY

Surface Intensity V^2/m^2:

$$I = \left| \sum_{\gamma=i,j,k} c_{i0,\gamma 1} \mathcal{E}_{\gamma 1} \right|^2 \tag{69}$$

Note: The superstrate indices, n_3 which yield the minimum in transmittance and the maximum in integrated surface intensity are labeled in (d).

SURFACE INTENSITY

Figure 20: Mapped surface intensity: (a) y component, (b) z component and (c) x component along 50 mm gold length for a superstrate index of 1.44 and (d) integrated surface intensity and transmittance for a $L = 200$ mm gold length vs. n_3 [2].

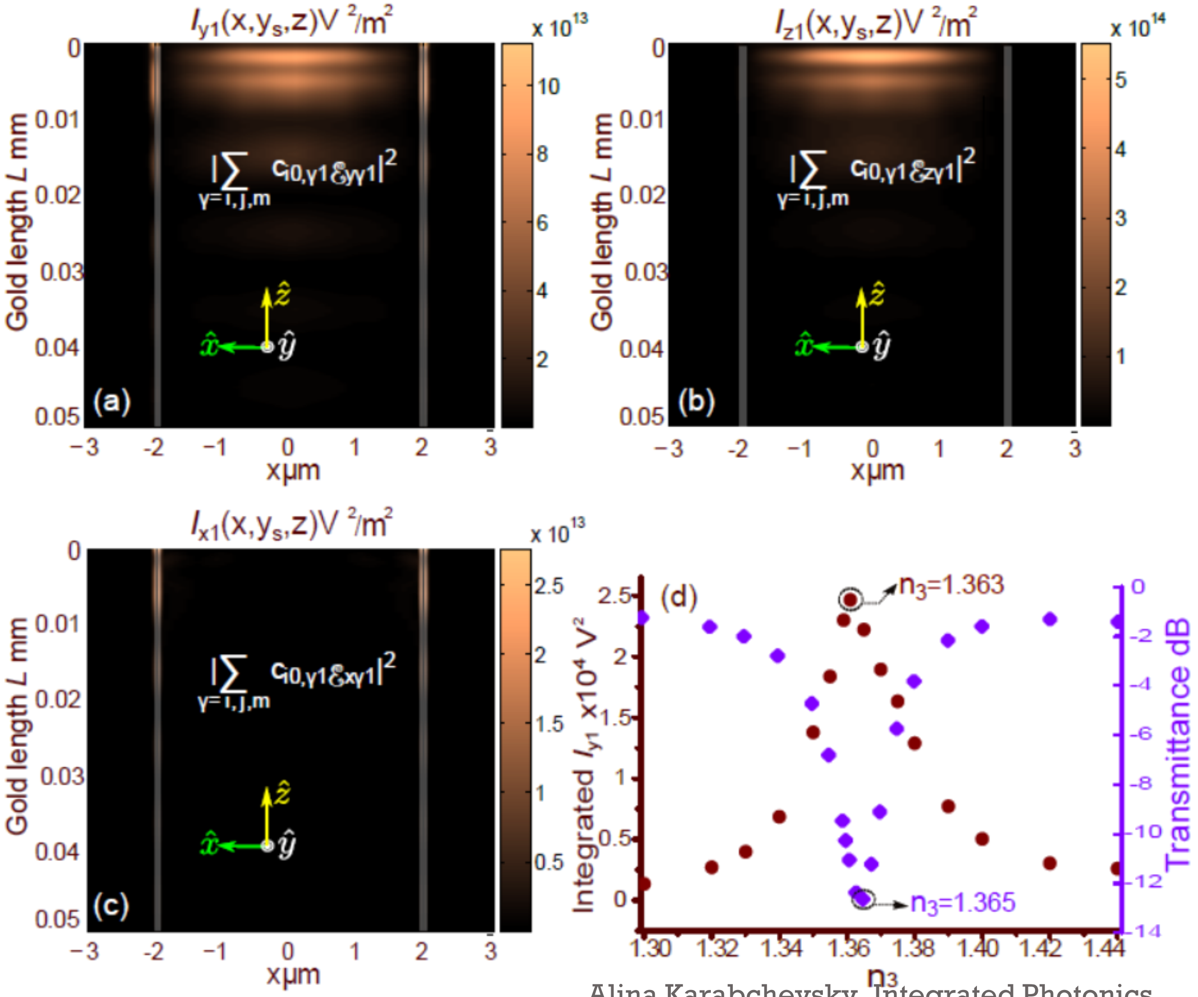

Alina Karabchevsky, James S Wilkinson, and Michalis N Zervas. Transmittance and surface intensity in 3d composite plasmonic waveguides. Optics express, 23(11):14407-14423, 2015.

CLOAKING WITH COMPOSITE PLASMONIC WAVEGUIDES

The interesting characteristics of composite plasmonic waveguides can be used to achieve novel devices. One of them is an invisibility cloak. Using transformation optics technique that is built upon two key observations:

- Maxwell's equations retain the same format under coordinate transformations in space, i.e. they are form-invariant under coordinate transformations.
- Maxwell's equations interpreted in different coordinate systems are equivalent to changing the medium parameters in the constitutive relationships.

TRANSFORMATION OPTICS

Consider a set of time-harmonic electric and magnetic fields $\tilde{\mathbf{E}}$ and $\widetilde{\mathbf{H}}$ at an angular frequency ω in a cartesian (x, y, z) coordinate system. Adopting the $e^{j\omega t}$ time convention, the fields satisfy Maxwell's curl equations at any source-free point.

$$\nabla' \times \tilde{\mathbf{E}}' = -j\omega\mu' \widetilde{\mathbf{H}}' \quad (70)$$

$$\nabla' \times \widetilde{\mathbf{H}}' = j\omega\varepsilon' \tilde{\mathbf{E}}' \quad (71)$$

where the constitutive relationships

$$\widetilde{\mathbf{B}} = \boldsymbol{\mu}\widetilde{\mathbf{H}} \qquad \widetilde{\mathbf{D}} = \boldsymbol{\varepsilon}\tilde{\mathbf{E}}$$

where $\widetilde{\mathbf{D}}$ and $\widetilde{\mathbf{B}}$ the electric and magnetic flux densities, respectively, $\boldsymbol{\varepsilon}$ is the electric permittivity tensor and $\boldsymbol{\mu}$ is the magnetic permeability tensor.

TRANSFORMATION OPTICS

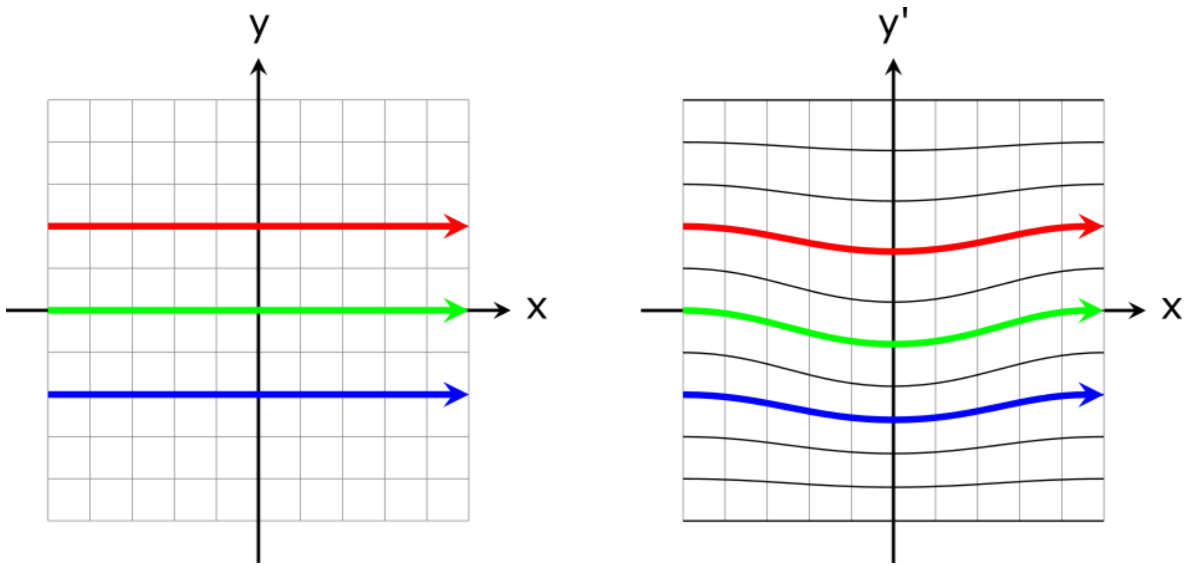

Since Maxwell's equations are form-invariant under coordinate transformations, the two curl equations in the transformed system may be written as:

$$\nabla' \times \tilde{\mathbf{E}}' = -j\omega\boldsymbol{\mu}'\tilde{\mathbf{H}}' \qquad (72)$$

$$\nabla' \times \tilde{\mathbf{H}}' = j\omega\boldsymbol{\varepsilon}'\tilde{\mathbf{E}}' \qquad (73)$$

TRANSFORMATION OPTICS

Let the coordinate transformation be described by the 3x3 Jacobian matrix A defined as:

$$\mathbf{A} = \begin{bmatrix} \partial x'/\partial x & \partial x'/\partial y & \partial x'/\partial z \\ \partial y'/\partial x & \partial y'/\partial y & \partial y'/\partial z \\ \partial z'/\partial x & \partial z'/\partial y & \partial z'/\partial z \end{bmatrix} \tag{74}$$

Both field and medium quantities in the (x', y', z') system are related to their respective counterparts in the (x, y, z) system. Specifically, the medium tensor parameters, μ_0' and ε_0', are related to μ_0 and ε_0 in the original space by the following expressions

$$\boldsymbol{\mu}' = \frac{\mathbf{A}\mu\mathbf{A}^T}{\det\{\mathbf{A}\}} \qquad \boldsymbol{\varepsilon}' = \frac{\mathbf{A}\varepsilon\mathbf{A}^T}{\det\{\mathbf{A}\}} \tag{75}$$

In addition, the fields in the transformed system are given in terms of the fields in the original system via

$$\tilde{\mathbf{E}}' = (\mathbf{A}^{-1})^T\tilde{\mathbf{E}} \qquad \tilde{\mathbf{H}}' = (\mathbf{A}^{-1})^T\tilde{\mathbf{H}} \tag{76}$$

THE COMPOSITE PLASMONIC WAVEGUIDE STRUCTURE

- Wavelength of $\lambda = 637$ nm illuminates the dielectric waveguide exciting the fundamental mode guided in region 0.
- Region 1 is characterized by the metasurface and Si nano-spacer placed on the waveguide with length L in the propagation direction exciting three hybrid plasmonic modes.
- Region 2 is identical to the region 0 in terms of the optical properties and functionality. A scattering object with optical index of 1.3 is placed on the metasurface.

THE COMPOSITE PLASMONIC WAVEGUIDE STRUCTURE

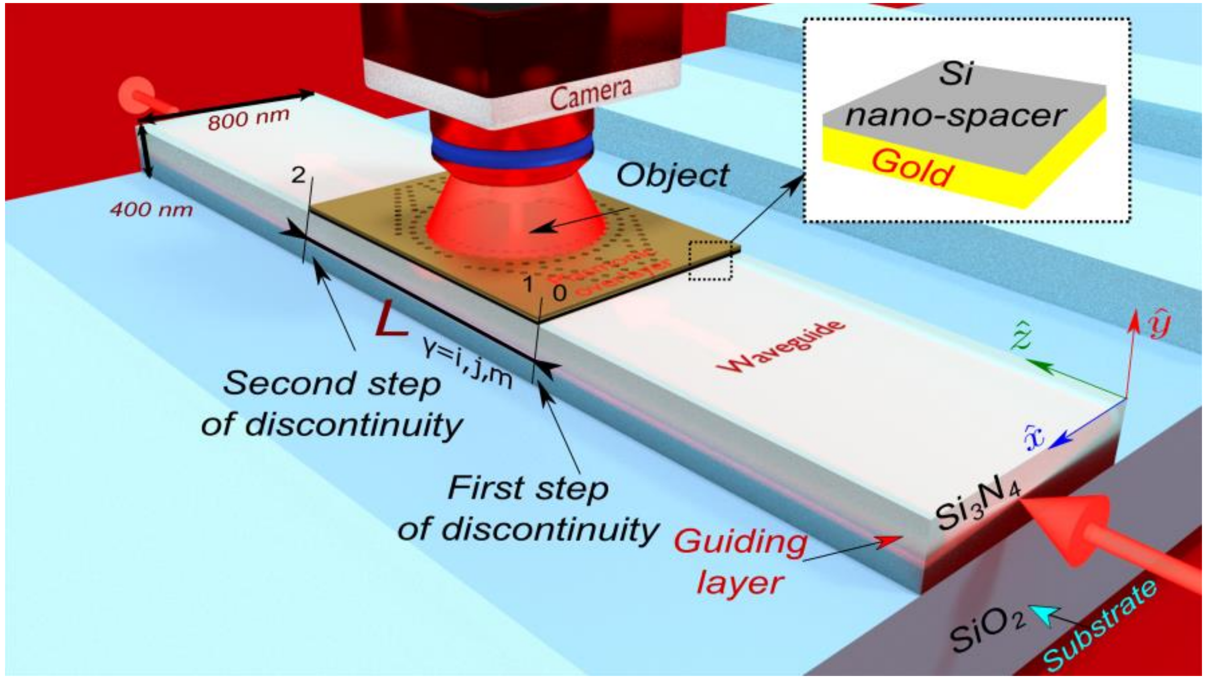

Figure 21: Illustration of the composite plasmonic waveguide structure and materials to study the invisibility cloaking scheme [3].

Yakov Galutin, Eran Falek, and Alina Karabchevsky. Invisibility cloaking scheme by evanescent fields distortion on composite plasmonic waveguides with si nano-spacer. Scientific reports, 7(1):12076, 2017.

COMPOSITE PLASMONIC WAVEGUIDE CLOAK DESIGN

If the mapping satisfies the Cauchy-Riemann conditions given by:

$$\partial x'/\partial x = \partial z'/\partial z \tag{77}$$

$$\partial x'/\partial z = \partial z'/\partial z \tag{78}$$

the transformed material becomes inhomogeneous and isotropic. The resulting transformation is composed of a quasi-orthogonal grid with an effective index in each cell:

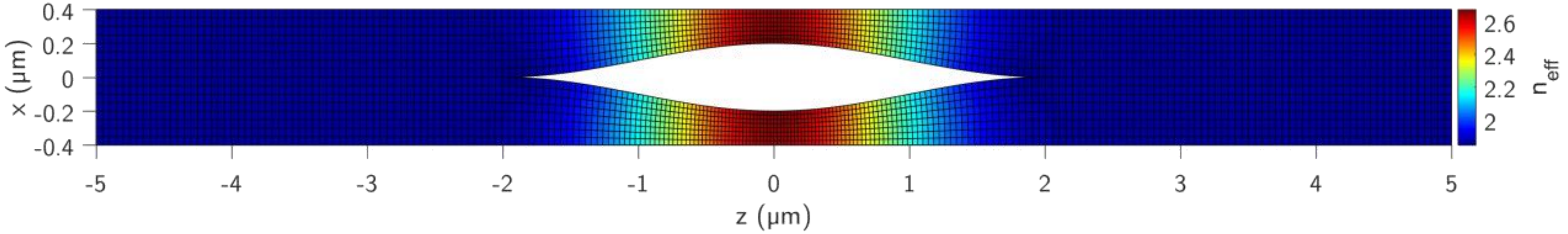

Figure 22: Transformed mesh using quasi-conformal transformation theme (black mesh) and calculated effective mode index, n_{eff} [3].

Yakov Galutin, Eran Falek, and Alina Karabchevsky. Invisibility cloaking scheme by evanescent fields distortion on composite plasmonic waveguides with si nano-spacer. Scientific reports, 7(1):12076, 2017.

CLOAKING RESULTS AND PERFORMANCE

The figure below shows calculated integrated total surface intensity to assess the effectiveness of evanescent invisibility cloak with a composite plasmonic waveguide.

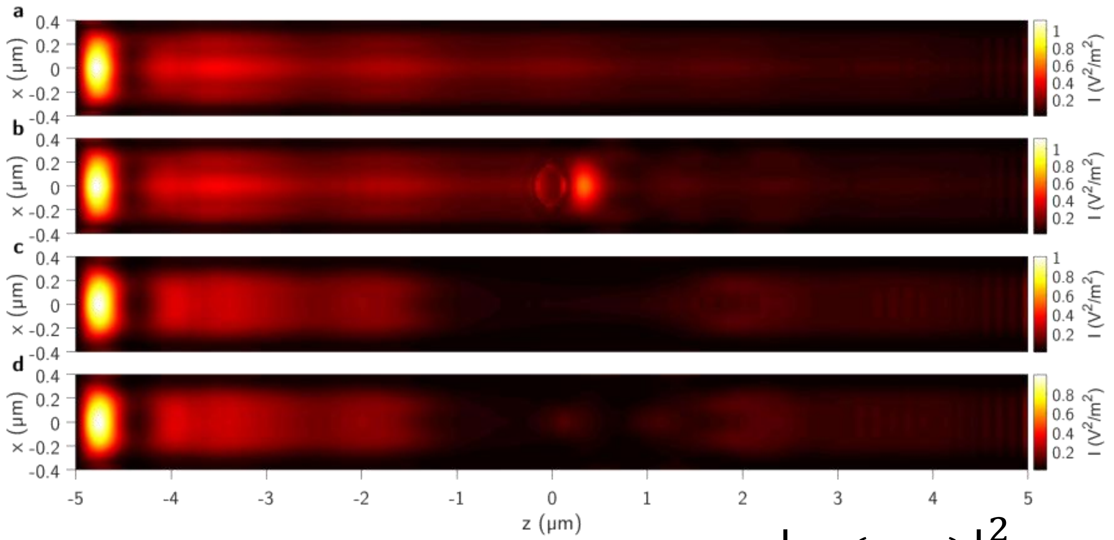

Figure 23: Calculated spatial surface intensities $|\varepsilon_y(x,y)|^2$ at $y = y_s$ in the composite plasmonic waveguide: (a) slab gold overlayer, (b) slab gold overlayer and an object index of 1.3, (c) transformed metasurface and (d) transformed metasurface and an object [3].

Yakov Galutin, Eran Falek, and Alina Karabchevsky. Invisibility cloaking scheme by evanescent fields distortion on composite plasmonic waveguides with si nano-spacer. Scientific reports, 7(1):12076, 2017.

BIBLIOGRAPHY: INTEGRATED PHOTONICS

[1] Alina Karabchevsky, Olga Krasnykov, Mark Auslender, Benny Hadad, Adi Goldner, and Ibrahim Abdulhalim. Theoretical and experimental investigation of enhanced transmission through periodic metal nanoslits for sensing in water environment. Plasmonics, 4(4):281, 2009.

[2] Alina Karabchevsky, James S Wilkinson, and Michalis N Zervas. Transmittance and surface intensity in 3d composite plasmonic waveguides. Optics express, 23(11):14407-14423, 2015.

[3] Yakov Galutin, Eran Falek, and Alina Karabchevsky. Invisibility cloaking scheme by evanescent fields distortion on composite plasmonic waveguides with silicon nano-spacer. Scientific reports, 7(1):12076, 2017.